Journal of Functional Foods 110 (2023) 105832

Contents lists available at ScienceDirect

Journal of Functional Foods

journal homepage: www.elsevier.com/locate/jff

Selenium nanoparticles functionalized by mushroom polysaccharide-protein complex: A novel nano-mineral for managing postmenopausal osteoporosis

Kar-Him Luk [a,b], Cheuk-Hin Chan [b], Zhi-Wen Liu [a], Chun-Wei Jiao [c], Xiao-Bing Yang [d], Xiao-Li Dong [a,b,*], Ka-Hing Wong [a,b,*]

[a] Research Institute for Future Food, The Hong Kong Polytechnic University, Hong Kong, China
[b] Department of Food Science and Nutrition, The Hong Kong Polytechnic University, Hong Kong, China
[c] Guangdong Yuewei Edible Fungi Technology Co., Ltd, Guangzhou, China
[d] Guangdong Institute of Microbiology, Guangzhou, China

ARTICLE INFO

Keywords:
Selenium nanoparticles
Postmenopausal osteoporosis
Mushroom polysaccharides-protein complex
Cordyceps sinensis
Nano-mineral

ABSTRACT

With an increase in aging population, osteoporosis has become one of the major public health issues nowadays, affecting over 200 million people worldwide. Since current medications are associated with various side effects, there is a clear clinical need to develop alternative therapeutics for managing osteoporosis. Selenium is an essential trace mineral, which has been proved to play important role in bone health. However, the narrow therapeutic window of selenium has greatly hindered its further development. Recently, selenium nanoparticles (SeNPs) have become a new selenium source due to its promising bioactivity and low toxicity. Nevertheless, scientific research concerning their effects on bone health is still very limited. By using the mushroom polysaccharide-protein complex isolated from *Cordyceps sinensis*, we have successfully prepared novel SeNPs ("Cs4-SeNPs") with well-characterized structure and high stability. Interestingly, Cs4-SeNPs (10 μM) were found to markedly induce proliferation, differentiation, and mineralization of the pre-osteoblast murine MC3T3-E1 cells. Further mechanistic study discovered that after cellular internalization via endocytosis, Cs4-SeNPs would trigger Nox4-derived intracellular ROS generation in the MC3T3-E1 cells followed by promoting downstream BMP-2 gene transcription and activating BMP signaling via both Smad dependent and Smad independent p38 MAPK pathways. More importantly, Cs4-SeNPs (25–500 μg/kg BW/d) exhibitedpromising *in vivo* bone protective efficacy against OVX-induced osteoporosis by promoting bone formation, inhibiting bone resorption, and improving bone microarchitecture after oral gavage for 6 weeks. Findings of this study collectively suggested that Cs4-SeNPs is of great potential to be further developed into a safe and evidence-based nano-mineral for managing postmenopausal osteoporosis.

1. Introduction

Osteoporosis is a metabolic bone disease characterized by low bone mass and deterioration of bone microarchitecture (Compston, McClung, & Leslie, 2019). The main clinical and public health concern of osteoporosis is its high risk of bone fractures, which may require hospitalization and even cause further morbidity or mortality because of prolonged immobilization (Compston et al., 2019). Osteoporosis is a serious public health concern, affecting more than 200 million people worldwide nowadays (Lorentzon et al., 2022). With the dramatic rise of world aging population by 2050, the cost on related surgery, hospital care and rehabilitation are expected to be tremendous, leading to significant medical and socioeconomic burdens (Lorentzon et al., 2022). Current medications for treating postmenopausal osteoporosis are classified into bone anti-resorptive and anabolic agents. Bisphosphonates, estrogens, and SERMs (e.g., raloxifene) are now the most commonly prescribed anti-resorptive drugs to reduce the risk of first and recurrent fractures of postmenopausal osteoporosis (An, 2016;

* Corresponding authors at: Room Y809, 8/F, Y Core, Department of Food Science and Nutrition, The Hong Kong Polytechnic University, Hung Hom, Kowloon, Hong Kong, China (Ka-Hing Wong). Room Y817, 8/F, Y Core, Department of Food Science and Nutrition, The Hong Kong Polytechnic University, Hung Hom, Kowloon Hong Kong, China (Xiao-Li Dong).
E-mail addresses: xiaoli.dong@polyu.edu.hk (X.-L. Dong), kahing.wong@polyu.edu.hk (K.-H. Wong).

https://doi.org/10.1016/j.jff.2023.105832
Received 27 July 2023; Received in revised form 6 October 2023; Accepted 8 October 2023
Available online 12 October 2023

Anagnostis et al., 2017; Black & Rosen, 2016; Notelovitz, 1997). However, side effects of the anti-resorptive therapy (e.g., higher risk of breast cancer) are of great concern (An, 2016; Anagnostis et al., 2017; Black & Rosen, 2016; Notelovitz, 1997). Parathyroid hormone (PTH) (e.g. teriparatide) is the only USFDA approved bone anabolic agent in current market. Due to its relatively high cost and inconvenience of daily subcutaneous injection, PTH has a restricted use for 24 months to patients with severe cases or glucocorticoid-induced osteoporosis (second line therapy) (Esbrit, Herrera, Portal-Núñez, Nogués, & Díez-Pérez, 2016; Sikon & Batur, 2010). Thus, there is a clear clinical need to develop alternative therapeutics for managing postmenopausal osteoporosis.

Selenium (Se) is an essential trace mineral to human health with a recommended daily allowance of 55 μg/day, playing important roles in many physiological functions (e.g., antioxidant) and pharmacological activities (e.g., anti-cancer) (Rayman, 2000). In the past decades, substantial research indicated that Se deficiency leads to bone microarchitecture damage and associated with osteoporosis, osteopenia, and Kashin-Beck osteoarthropathy (Cao, Gregoire, & Zeng, 2012; Regina Ebert & Jakob, 2007; Moreno-Reyes, Egrise, Nève, Pasteels, & Schoutens, 2001; Moreno-Reyes et al., 2003), indicating its important role in bone health. Previous research demonstrated that Se supplementation could not only enhance the anti-oxidative capacity to prevent cell damage in bone marrow stromal cell, but also against the H_2O_2-induced inhibition of osteoblastic differentiation via suppressing oxidative stress and ERK signaling pathways (R. Ebert et al., 2006; Liu, Bian, Liu, & Huang, 2012). Nevertheless, the narrow therapeutic window of Se greatly hinders its biomedical application in bone health. Recently, selenium nanoparticles (SeNPs) have become a new Se source, as they were found to possess promising bioactivity and lower toxicity than selenocompounds commomly found in foods (e.g. selenite) (Chaudhary, Umar, & Mehta, 2014; Ferro, Florindo, & Santos, 2021; H. Wang, Zhang, & Yu, 2007; J. Zhang, Wang, Yan, & Zhang, 2005). However, scientific research relating their effects on bone health is currently very limited (S. Yu et al., 2018; Zheng et al., 2014). Besides, SeNPs aggregate easily and their bioactivity will be markedly diminished, if its nano size could not be maintained. This limiting factor has attracted many scientists to search for substances that could improve the stability of SeNPs without copromising their health-promoting efficacy.

Cordyceps sinensis (Berk.) Sacc. is a precious medicinal fungus, which has been used as a tonic food and therapeutic herb in China for more than 700 years (Zhu, Halpern, & Jones, 1998a, 1998b). As wild *C. sinensis* is very rare and expensive, successfully cultivation of its fourth isolated mycelia (Cs4) by Chinese Academy of Sciences has undoubtedly facilitated the scientific research on this special strain in the past decades. Substantial pharmacological and clinical studies have demonstrated that polysaccharide protein complex (PSP) is one of the major bioactive constituents of Cs4, exhibiting a wide range of health-promoting and therapeutic efficacy such as immunomodulation, anti-tumor, antioxidant, in particular anti-osteoporosis (Qi et al., 2012; Shashidhar, Giridhar, & Manohar, 2015; Yan, Wang, & Wu, 2014).

By using different mushroom PSP, we have successfully prepared various SeNPs with well-characterized structure and health-promoting activity (G. Huang et al., 2018; S. Yu et al., 2018; Zeng et al., 2019). In this study, we rationally designed a novel SeNPs ("Cs4-SeNPs") functionalized with the Cs4 PSP, which has been found to possess anti-osteoporosis efficacy. Aside from cellular uptake behavior, we investigated the bone stimulating effects of Cs4-SeNPs *in vitro* followed by elucidation of their mechanism of action in regulating the BMP signaling cascades during osteoblast differentiation. Besides, the *in vivo* bone protective efficacy of Cs4-SeNPs against ovariectomy-induced osteoporosis was also evaluated.

2. Materials and methods

2.1. Chemicals and reagents

Crude Cs4 polysaccharide-protein complex (Cs4 PSP) was purchased from Johncan International (Hangzhou, China). All chemicals used were analytical grade and purchased from Sigma-Aldrich (Saint Louis, Missouri, USA). 4′,6-diamidino-2-phenylindole (DAPI) and Lysotracker Deep Red were purchased from Invitrogen (San Diego, CA, USA). MTS assay kit was purchased from Promega (USA). Primary antibodies including BMP-2, p-Smad 1/5/8, Smad 1/5/8, p-ERK, ERK, p-p38, p-38, p-JNK, JNK, GAPDH and secondary anti-mouse IgG were purchased from Cell Signaling Technology (USA). Mouse OCN ELISA kit was purchased from LifeSpan BioScience Inc. (USA); DCFDA Cellular ROS Detection Assay Kit, ALP Assay Kit and Acid Phosphatase Assay Kit were purchased from Abcam (USA).

2.2. Cell culture and animal

Murine MC3T3-E1 subclone 4 pre-osteoblasts were purchased from American Type Culture Collection (ATCC ® CRL-2593, Rockville, MD, USA) and maintained in ascorbic acid free α-Minimum Essential Medium (α-MEM; Invitrogen, San Diego, CA, USA) supplemented with 10% fetal bovine serum (FBS; Invitrogen, San Diego, CA, USA), 1% 100 × antibiotics and anti-mycotics (Invitrogen, San Diego, CA, USA) in a 37 °C incubator with 95% relative humidity and 5% CO_2. 3-month-old female C57BL/6J mice were purchased from The Chinese University of Hong Kong and housed in pathogen-free isolation facilities with a light/dark cycle (12/12 h), temperature (24.0 ± 1 °C); and humidity (65.0 ± 5%) control. All animal procedures were performed in accordance with the Guidelines for Care and Use of Laboratory Animals and approved by the Animal Subjects Ethics Sub-Committee of The Hong Kong Polytechnic University (Case No. 16–17/43-ABCT-R-OTHERS).

2.3. Preparation and characterization of Cs4-SeNPs

Standardized Cs4-SeNPs (Se concentration: 1.43 ± 0.11 mM) were prepared using our patented nanotechnology (China patent no.: CN201911215358.5). In brief, aqueous Cs4 PSP (0.25%) were mixed with freshly prepared ascorbic acid (100 mM) under magnetic stirring prior to drop-wise addition of aqueous sodium selenite (25 mM). After reconstituting with MiliQ water to 25 mL, the mixture reacted under room temperature with stirring for 12 hrs followed by extensive dialysis (*M*w cutoff: 8,000 Da). Chemical composition and structure of the resulting Cs4-SeNPs were further characterized by ICP-OES (Agilent 710; Agilent Technologies Inc., Santa Clara, CA, USA), Nanosight NS300 and Zetasizer Nano ZS particle size analyzer (Malvern Instruments Ltd., UK), TEM (H-7650; Hitachi, Japan), HR-TEM-EDX (JEM-2100F; JEOL + EX-250; Horiba, Japan) and FT-IR (Equinox 55, Bruker, Germany) as described previously (G. Huang et al., 2018; Hualian Wu et al., 2012; H. Wu et al., 2013).

2.4. In vitro stimulating effects of Cs4-SeNPs on osteogenesis

For cell proliferation, MC3T3-E1 cells were firstly seeded into 96-well tissue culture plates at 15,000 cells/well. Cells were then incubated with different concentrations of Cs4-SeNPs (0.1 nM-20 μM), Cs4-PSP (6 μg/mL), sodium selenite (10 μM) and selenomethionine (10 μM) in ascorbic acid free α-MEM supplemented with 10% FBS, 1% 100 × antibiotics and antimycotics in a 37 °C incubator with 95% relative humidity and 5% CO_2 for 24, 48 and 72 hrs. The cell proliferation was investigated and compared by using MTS assay, while the most effective dosage of Cs4-SeNPs was determined and used for subsequent *in vitro* experiments. For osteoblast differentiation, MC3T3-E1 cells were cultured in osteogenic medium consisting of 50 μg/mL ascorbic acid and 10 mM β-glycerophosphate and pretreated for 6 days with the Cs4-

SeNPs (10 μM). Freshly prepared osteogenic medium was replaced every 3 – 4 days. ALP activity in the MC3T3-E1 cells was determined by spectrophotometry at 405 nm, while ALP-containing cells (osteoblasts) were visualized by ALP staining kit. For bone mineralization, bone nodules formed in MC3T3-E1 cells after treatment with the Cs4-SeNPs (10 μM) for 18 days were visualized and compared by both Von Kossa and Alizarin Red S staining as previously described (Kim, Kang, Park, & Lee, 2015; S. Yu et al., 2018).

2.5. Mechanistic study of the stimulating effects of Cs4-SeNPs on osteoblastic differentiation

2.5.1. Cellular uptake behavior

To determine the cellular uptake behavior of CS4-SeNPs, coumarin-6-loaded Cs4-SeNPs were prepared as previously described (B. Yu, Zhang, Zheng, Fan, & Chen, 2012). In brief, MC3T3-E1 cells were seeded in a 35 mm confocal dish for 24 hrs followed by sequential staining with Hochest 33,342 (1 μg/mL; 20 min) and Lysotracker Deep Red (75 μM; 30 min). The intracellular uptake behavior of coumarin-6-loaded Cs4-SeNPs (10 μM) was traced after incubation at 37 °C for different periods of time (0–14 min) using fluorescence microscopy (Zeiss Lightsheet Z.1 Microscope, Germany) as described previously (S. Yu et al., 2018).

2.5.2. In vitro modulation effects of Cs4-SeNPs on BMP signaling

To figure out the involvement of BMP/Smad dependent and/or independent pathways in Cs4-SeNPs mediated osteoblast differentiation, MC3T3-E1 cells cultured in osteogenic medium containing β-glycerophosphate (10 mM) and ascorbic acid (50 μg/mL) were firstly pretreated with Cs4-SeNPs (10 μM) for 3, 6, 9 and 18 days. Protein expression and phosphorylation of BMP-2, Smad 1/5/8 and MAPKs kinases (including p38, JNK and ERK) were then quantified by Western blot analysis while mRNA expression of major osteogenic biomarkers such as ALP, Dlx5, Runx2, Osx and OCN was obtained by real-time PCR analysis as reported previously (Rossouw et al., 2002; S. Yu et al., 2018). In order to confirm whether BMP/Smad dependent and/or independent pathways is mechanistically linked to the Cs4-SeNPs mediated osteoblast differentiation, the effects of Noggin (10 ng/mL; BMP signaling inhibitor), SB258530 (10 μM; p38 inhibitor), SP600125 (10 μM; JNK inhibitor) and U0126 (10 μM; ERK inhibitor) on the ALP activity, mRNA expression of major osteogenic biomarkers (such as Dlx5, Runx2 and Osx) as well as bone nodule formation (Von Kossa and Alizarin Red S staining) were further investigated in the MC3T3-E1 cells as previously reported (Rossouw et al., 2002; S. Yu et al., 2018).

2.5.3. Nox4 derived intracellular ROS generation

Intracellular ROS generation triggered by Cs4-SeNPs in the MC3T3-E1 cells was detected using the DCFDA Cellular ROS Detection Assay Kit (ab113851, Abcam, UK) according to manufacturer's instructions. In brief, MC3T3-E1 cells pretreated with Cs4-SeNPs (10 μM) or 50 μM *tert*-butyl hydrogen peroxide (TBHP; positive control) for 24 hrs were stained with DCF-DA for 45 min at 37 °C in dark prior to visualization under fluorescence microscopy (Zeiss Lightsheet Z.1 Microscope, Germany). Besides, mRNA expression of Nox4 in MC3T3-E1 cells pretreated with Cs4-SeNPs (10 μM) for 3 days was quantified by real-time PCR.

2.5.4. Total RNA isolation

In brief, cells and bone tissues were washed with PBS prior to total RNA extraction using 1 mL of Trizol reagent in accordance with the manufacturer's instructions (Life technologies, USA). After homogenization, 200 μL of chloroform was added to the samples with moderate shaking before standing at room temperature for 3 min. All samples were then centrifuged at 12,000 × g for 15 min at 4 °C followed by transferring the upper layer into a new centrifuge tube. After sequential washing with 2-propanol and 75% ethanol, the RNA pellet was air-dried. Once the RNA pellets turned into milky, 10 – 20 μL of DEPC treated water was added to re-dissolve the RNA and stored at −80 °C until further real-time PCR analysis.

2.5.5. Real-time polymerase chain reaction (qPCR)

In short, 20 ng of RNA was firstly prepared by One-Step SYBR Green RT-qPCR according to manufacturer's instructions. The reaction mixture for a 20 μL reaction includes 10 μL of 2X One Step TB Green RT-PCR Buffer 4, 0.8 μL of PrimeScript 1 Step Enzyme Mix 2, 0.4 μM of PCR forward primers, 0.4 μM of PCR reverse primers, 0.4 μL ROX Reference Dye II and 20 ng of RNA sample. Major osteogenic markers including ALP, DLx5, Runx2, Osx, and OCN were analyzed by qPCR using Applied Biosystems QuantStudio™ 7 Flex Real-Time PCR System (Thermo, USA) and corresponding PCR reaction conditions and primer sequences are described in **Supplementary Tables S1 and S2**, respectively. Relative mRNA expression of each osteogenic marker gene was normalized to that of GAPDH (*in vitro* study) or β-actin (*in vivo* study).

2.5.6. Total protein extraction

In brief, after removing the culture medium, the cells were washed twice with cold PBS followed by adding 200 μL of cold RIPA Lysis Buffer containing PMSF and phosphatase inhibitor cocktail. Cells lysis solution was then transferred into 1.5 mL microcentrifuges tube followed by centrifugation at 14,000 × g for 30 min at 4 °C to collect the protein extracts. Protein concentration of the supernatant was determined by BCA kit assay. After mixed with 5X sample buffer, the reaction mixture was heated up to 95 °C for 5 min and stored at −20 °C prior to Western blot analysis.

2.5.7. Western blot analysis

In short, equal amounts of protein extracts (40 μg) were firstly loaded into and separated by 10% SDS-PAGE electrophoresis. Separated proteins were then electro-transferred to PVDF membranes. After blocking with 5% BSA for 1 hr at room temperature, the membranes were incubated with specific primary antibodies at 4 °C overnight. Following several washes with TBST, the membranes were incubated with horseradish peroxidase (HRP)-conjugated secondary antibodies for 1 hr at room temperature. Subsequently, the membranes were washed with TBST, and protein bands were detected with an enhanced chemiluminescence (ECL) reagent kit (Millipore, USA) using a AzureTM C600 digital imager (Azure Biosystem Inc., USA) followed by quantification with ImageJ software.

2.6. In vivo bone protective efficacy of Cs4-SeNPs against postmenopausal osteoporosis

In brief, 3-month-old mature, female C57BL/6J mice were either OVX or sham operated. After recovery from surgery for 2 weeks, all mice were randomly assigned to 6 different groups followed by treatment with Cs4-SeNPs and 17β-estradiol (E2; positive control) for a total of 6 weeks:

Group 1: Sham + vehicle (Sham; Milli Q water/day; oral gavage; n = 8);

Group 2: OVX + vehicle (OVX; Milli Q water/day; oral gavage; n = 8);

Group 3: OVX + E2 (1 mg/kg BW/day; 5 days per week; oral gavage; n = 8) (L. Huang et al., 2018);

Group 4: OVX + Cs4-SeNPs (25 μg Se/kg BW/day; oral gavage; n = 8);

Group 6: OVX + Cs4-SeNPs (250 μg Se/kg BW/day; oral gavage; n = 8); and.

Group 7: OVX + Cs4-SeNPs (500 μg Se/kg BW/day; oral gavage; n = 8).

During the experiment, mice were paired with standard rodent laboratory chow and their body weight were recorded weekly. All animals had free access to distilled water and diet. At the end of the 6 weeks treatment period, all mice were euthanized for collecting cardiac blood

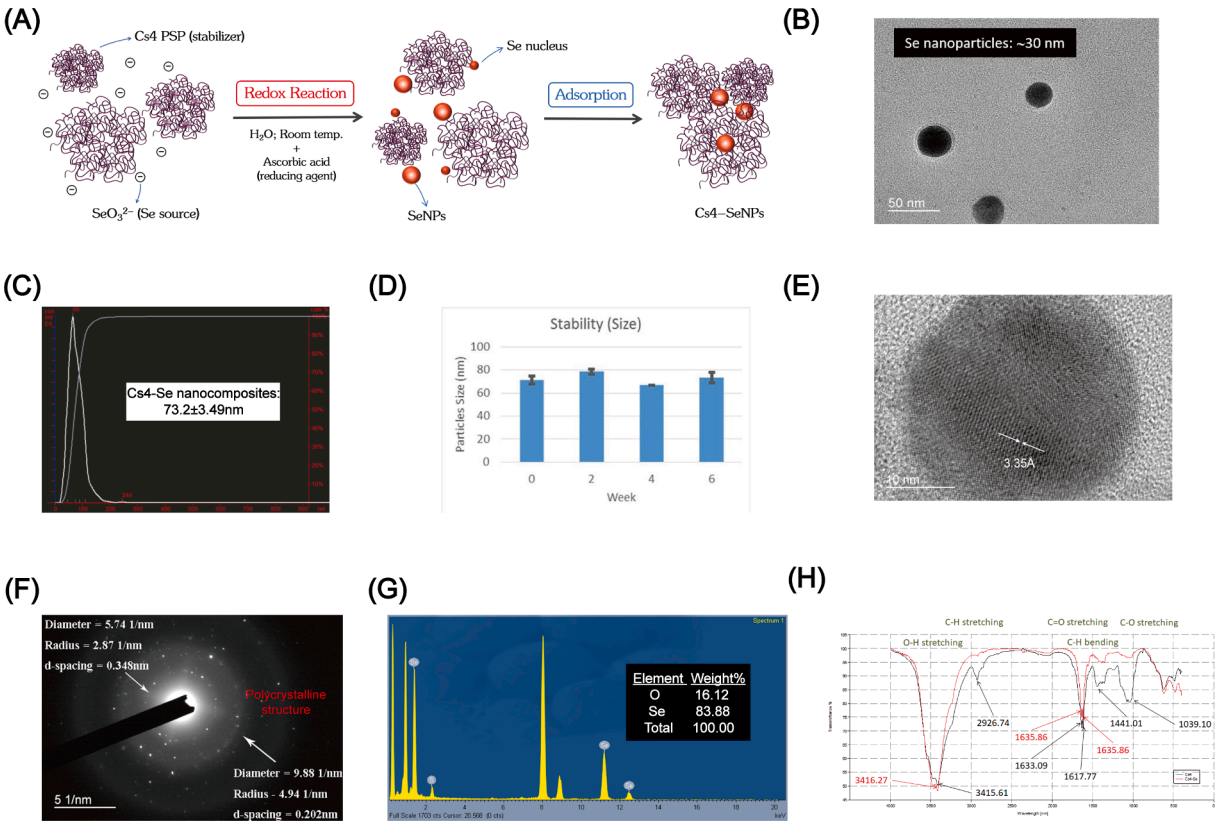

Fig. 1. Preparation and characterization of Cs4-SeNPs. (A) A schematic diagram of Cs4-SeNPs preparation. (B) Representative TEM image. (C) Particles size distribution. (D) Particles size stability. (E) Representative HR-TEM image showing lattice fringes and (F) SAED pattern. (G) EDX spectrum. (H) FT-IR spectrum.

samples. Blood samples were then centrifuged for serum isolation and stored at −80 °C prior to bone turnover markers analysis. Proximal femurs and fifth lumbar vertebra were dissected for measurement of trabecular microarchitecture. The left tibia was collected to determine mRNA expression of Runx2 and Osx using real time-PCR, while the uterus was excised and weighed to calculate the uterus/body weight ratio.

2.6.1. Micro-computed tomography (MicroCT) analysis

The proximal femurs and the fifth lumbar vertebra were scanned by microCT system (μCT-40; Scanco Medical, Switzerland), with a voxel size of 16.4 mm. 80 continuous slices starting at 0.3 mm from the most distal aspect of the growth plate and extending distally along the femur diaphysis were selected for analysis in the proximal femur. For 3-D reconstruction, all the trabecular bone from each selected slice was segmented (Sigma = 1.2, Supports = 2 and Threshold = 220) to calculate bone mineral density (BMD), trabecular separation (Tb.Sp), bone volume/tissue volume ratio (BV/TV), trabecular thickness (Tb.Th), and trabecular number (Tb.N) (X. Wang et al., 2015).

2.6.2. Analysis of bone turnover markers

Bone turnover was assessed by determining serum ALP level (bone formation marker) and tartrate-resistant acid phosphate (TRAP) activity (bone resorption marker) using colorimetric assay kits (ab83369 and ab83367, Abcam, USA) according to manufacturer's instructions.

2.7. Statistical analysis

All data were presented as mean ± standard error of mean (SEM). The mean values were analyzed by one-way ANOVA and Tukey-HSD to detect significant difference among groups using GraphPad PRISM version 4.0 (GraphPad Software, San Diego, CA, USA). A difference with $P < 0.05$ (*), $P < 0.01$ (**) and $P < 0.001$ (***) was considered statistically significant.

3. Results and discussions

3.1. Preparation and characterization of Cs4-SeNPs

By using the Cs4 PSP as capping agent, standardized Cs4-SeNPs (Se concentration: 1.35 ± 0.12 mM) were successfully prepared under a redox reaction using our patented nanotechnology (China patent no.: CN201911215358.5; Fig. 1**A**). Further structure characterization indicated that Cs4-SeNPs existed as uniform and mono-dispensed spherical particles with an average core size of around 30.0 nm (Fig. 1**B**). Similar findings on shape and core particle size (ranged from 12.5 − 20 nm) of other mushroom PSP decorated SeNPs have been reported previously (Zeng et al., 2019). Besides, Cs4-SeNPs display high stability in aqueous solution without obvious change in its hydrodynamic size (73.2 ± 3.49 nm) over 6 weeks (Fig. 1**C & 1D**). For individual SeNPs, the clear lattice fringes/d-spacing (3.35 Å), SAED pattern (diffuse rings constructed with white dots) as well as EDX elemental composition collectively suggested that the resulting nanoparticle possessed a polycrystalline structure with high level of Se (about 84%) (Fig. 1**E, 1F & 1G**). As shown in the FT-IR spectrum (Fig. 1**H**), Cs4 PSP shared a very similar FT-IR spectrum to that of Cs4-SeNPs, indicating a successful surface decoration of SeNPs by Cs4 PSP. Besides, the absorption peaks at wavelengths 1617 cm^{-1} and 1633 cm^{-1} indicated the presence of amine (N-H bending) in protein moiety of Cs4 PSP, while the absorption peak at wavelength 3415 cm^{-1} indicated the abundance of the stretching vibrations of hydroxyl (–OH–) groups of its polysaccharides. As reported by Zeng et al. (Zeng et al., 2019), both amine and hydroxyl groups in mushroom PSP could effectively bind to SeNPs, resulting in a high stability of SeNPs in aqueous solution.

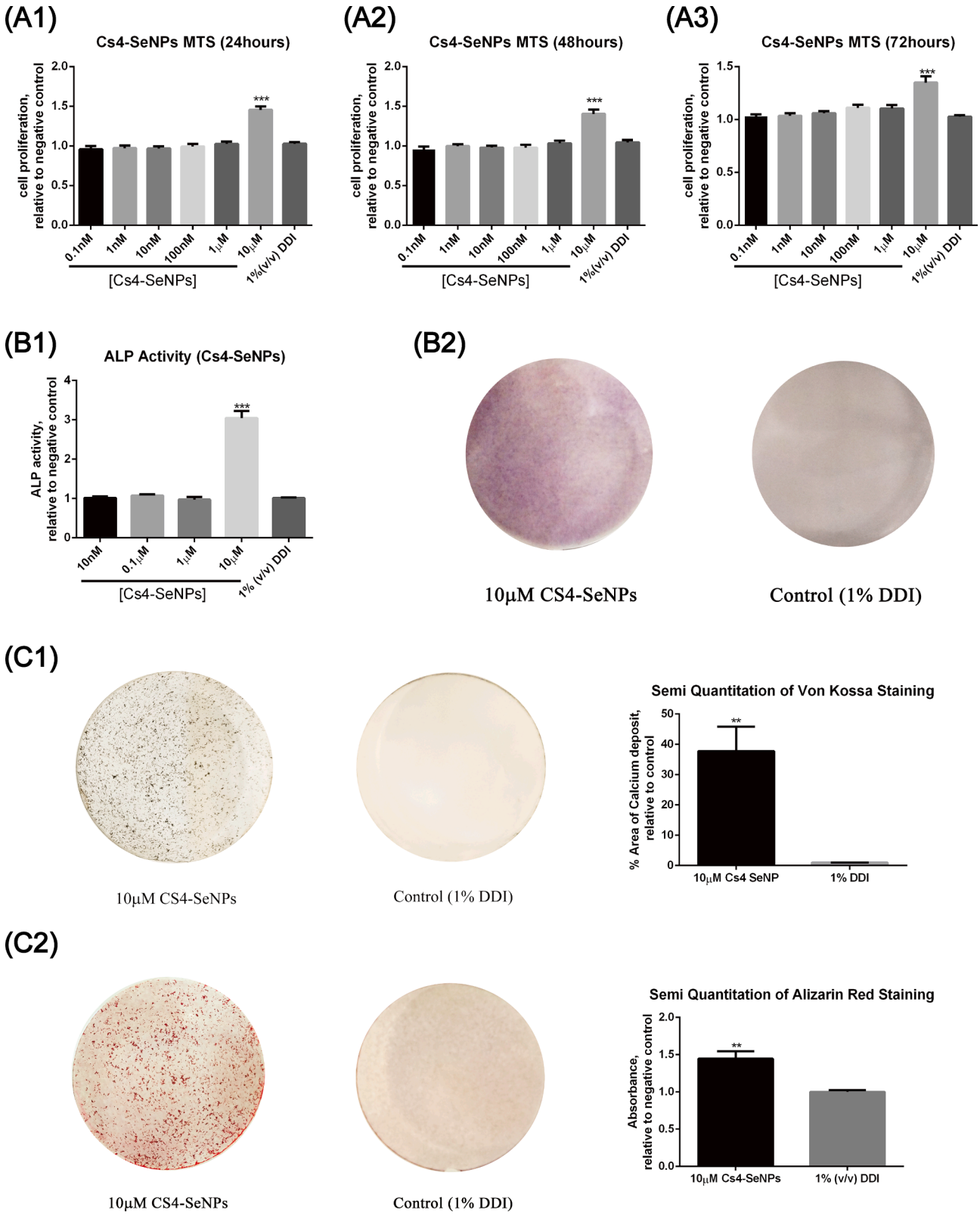

Fig. 2. Cs4-SeNPs stimulated proliferation, differentiation, and bone mineralization of MC3T3-E1 cells. (A) Cell proliferation was determined using an MTS assay after MC3T3-E1 cells treated with Cs4-SeNPs (0.1 nM – 10 μM) for (A1) 24, (A2) 48 and (A3) 72 hrs. Normalized results were compared with that of the negative control group (1% deionized water; DDI). For differentiation, MC3T3-E1 cells were treated with different concentrations of Cs4-SeNPs (10 nM-10 μM) in osteogenic medium for 6 days; (B1) Cells were subjected to ALP activity measurement, normalized results were compared with that of the negative control group (1% deionized water; 1 %DDI); (B2) Cells were subjected to ALP staining. For bone mineralization, after 18 days of treatment with 10 μM Cs4-SeNPs in osteogenic medium on MC3T3-E1 cells, matrix mineralization was visualized using Von Kossa staining (C1) and Alizarin Red S staining (C2). Results are mean ± SEM (n = 3). Means with "**" and "***" are significantly different at $p < 0.01$ and $p < 0.001$, respectively. (For interpretation of the references to colour in this figure legend, the reader is referred to the web version of this article.)

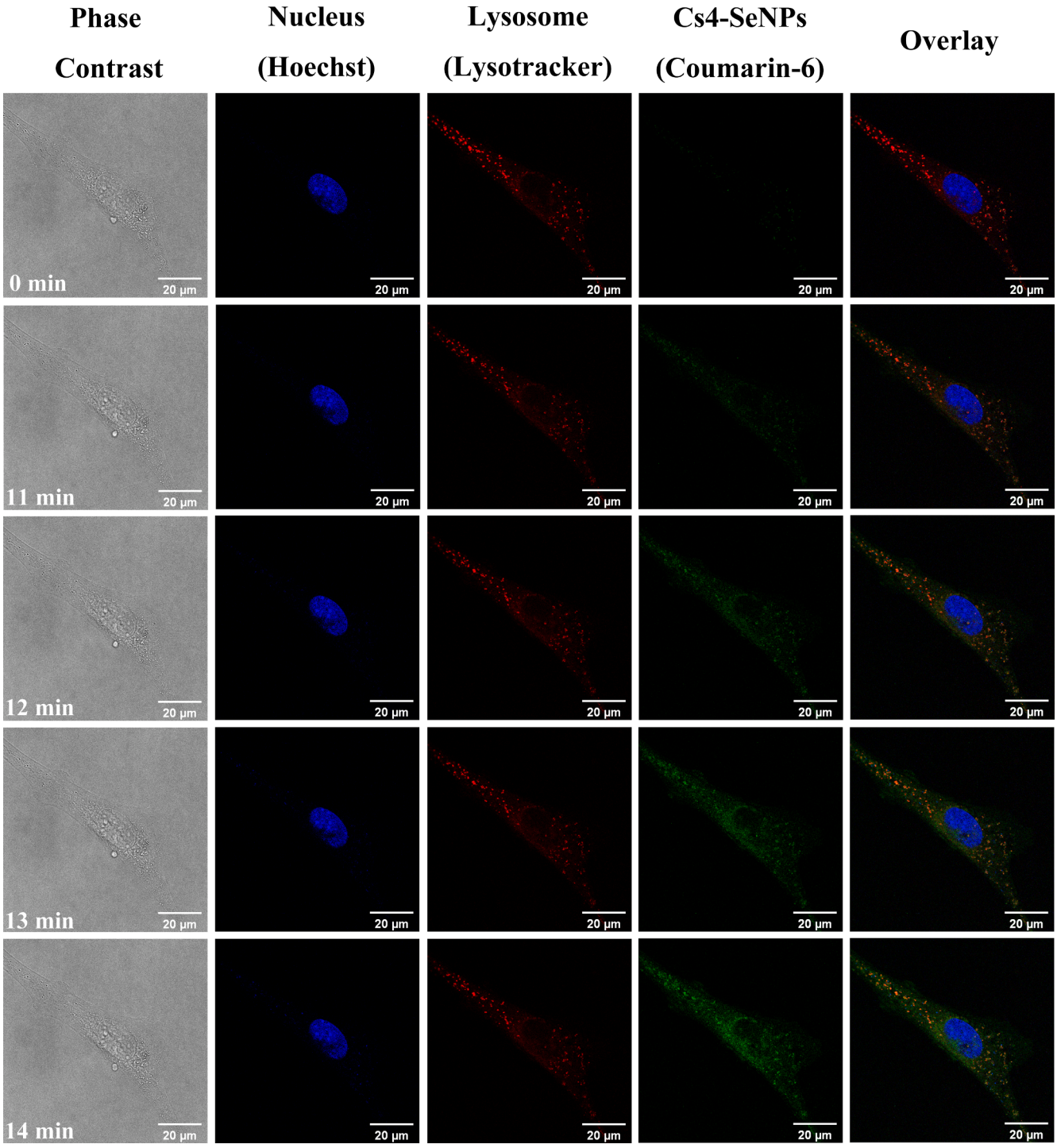

Fig. 3. Cellular uptake behavior of Cs4-SeNPs in MC3T3-E1 cells. MC3T3-E1 cells were sequentially stained with Hochest 33,342 (1 μg/mL; 20 min; blue) and Lysotracker Deep Red (75 μM; 30 min; red). After incubation with the coumarin-6-loaded Cs4-SeNPs (10 μM; green) for different time intervals (0–14 min) at 37 °C, the cellular uptake behavior was visualized by fluorescence microscopy (Scale bar: 20 μm). (For interpretation of the references to colour in this figure legend, the reader is referred to the web version of this article.)

3.2. Cs4-SeNPs stimulate proliferation, differentiation, and bone mineralization of MC3T3-E1 cells

The direct effects of Cs4-SeNPs on proliferation, differentiation, and bone mineralization of murine MC3T3-E1 subclone 4 pre-osteoblasts were characterized. Interestingly, Cs4-SeNPs was found to significantly enhance the proliferation of MC3T3-E1cells (1.35 – 1.45 folds) after 24, 48 and 72hrs treatment with 10 μM of Cs4-SeNPs (Fig. 2**A1-A3** & **Fig. S1**). Alkaline phosphatase (ALP) is a widely used phenotypic biomarker for osteoblastic differentiation. As shown in Fig. 2**B1&2**, Cs4-SeNPs significantly stimulated the differentiation of MC3T3-E1 cells after 6-day treatment as indicated by a notably increase in ALP activity (3.05 folds, Fig. 2**B1**) and ALP containing cells (with purple-blue colors by ALP staining; Fig. 2**B2**). For bone mineralization, Cs4-SeNPs (10 μM) markedly induced mineralized nodule formation in the MC3T3-E1 cells (1.45 ± 0.12 folds) as determined by Von Kossa and Alizarin Red S staining (Fig. 2**C1&2**). It is worth noting that with a remarkable low effective dosage (10 μM only), Cs4-SeNP triggered faster differentiation

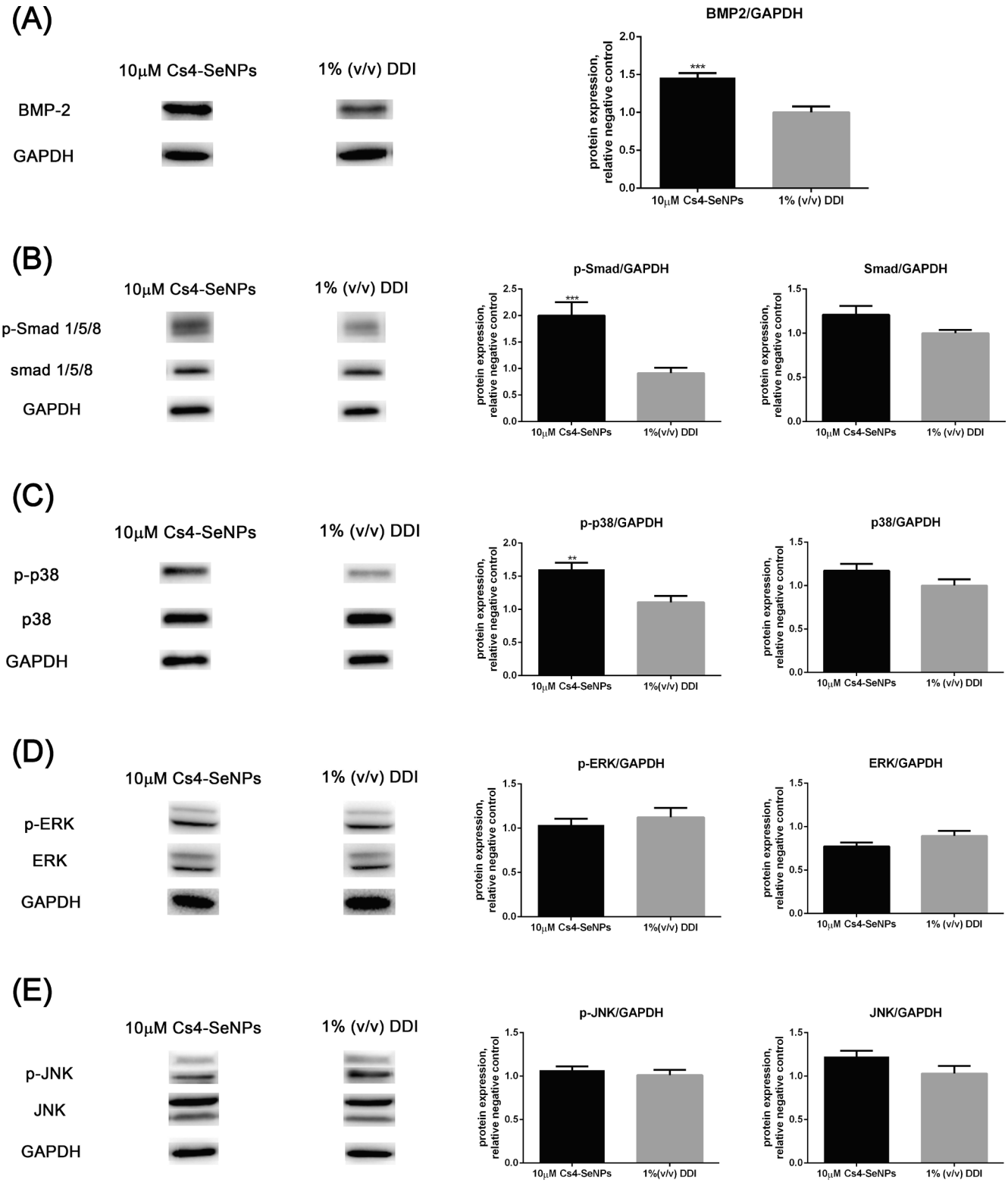

Fig. 4. Cs4-SeNPs induced osteoblastic differentiation in MC3T3-E1 cells by activating BMP-2/Smad dependent and independent pathways. Cells were induced with osteogenic medium for 3 days with Cs4-SeNPs (10 μM) or 1% (v/v) DDI, protein expression of (A) BMP-2, (B) p-Smad 1/5/8 and Smad 1/5/8, (C) p-p38 and p38, (D) p-ERK and ERK and (E) p-JNK and JNK were quantified by Western blot analysis and normalized to that of GAPDH. Results are mean ± SEM (n = 3). Means with "**" and "***" are significantly different at $p < 0.01$ and $p < 0.001$, respectively.

(6 days) and bone mineralization (18 days) of the MC3T3-E1 cells when compared with those of other SeNPs (effective dosage: 63.3–126.5 μM; osteoblast differentiation: 14 days; bone mineralization: 28 days) (Lee et al., 2021). The possible contribution of Cs4 PSP surface decoration (6 μg/mL) to the *in vitro* bone stimulating effect of Cs4-SeNPs was further investigated. As shown in Figs. S2-S4, Cs4 PSP alone exhibited insignificant effect on the osteogenesis of MC3T3-E1 cells, suggesting that SeNPs itself would likely be the major active component of Cs4-SeNPs.

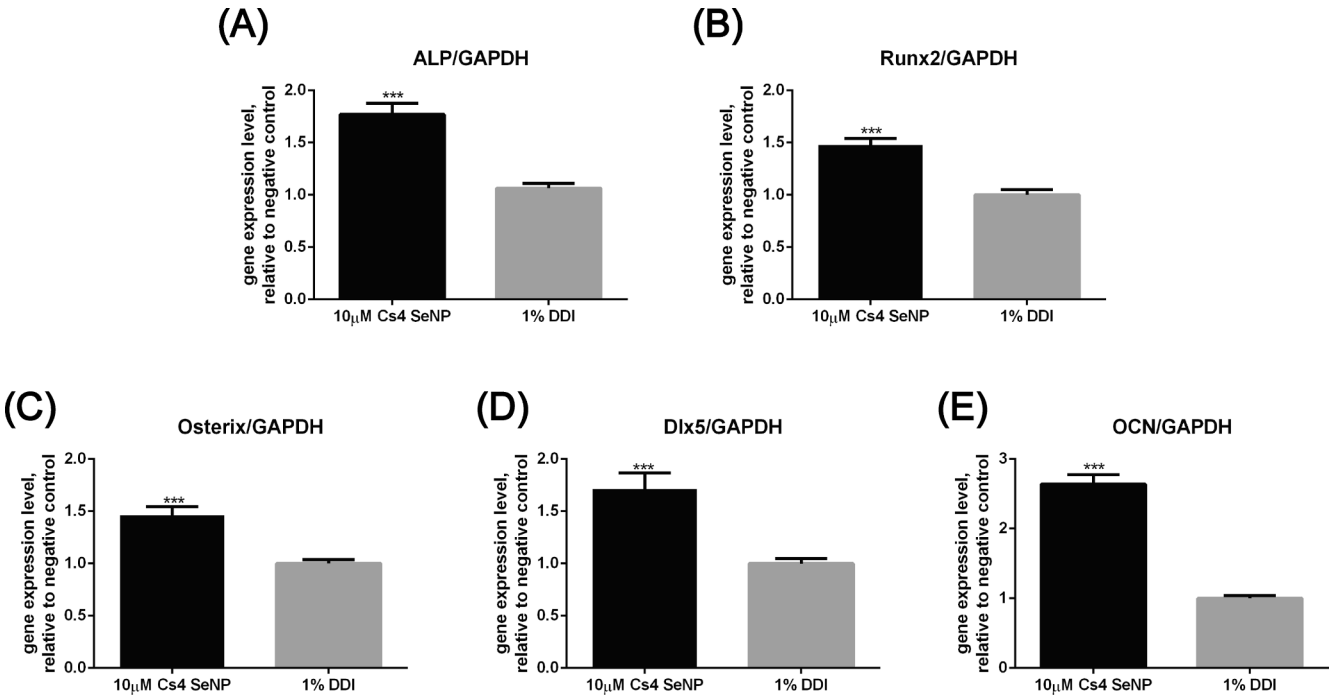

Fig. 5. Cs4-SeNPs upregulated mRNA expression of major osteogenic markers in MC3T3-E1 cells. Cells were induced with osteogenic medium for 6 or 9 days with Cs4-SeNPs (10 μM) or 1% (v/v) DDI, expression of (A) ALP, (B) Runx2, (C) Osx, (D) Dlx5 and (E) OCN at the mRNA levels was determined by qPCR analysis and normalized to that of GAPDH. Results are mean ± SEM (n = 3). Means with "***" are significantly different at $p < 0.001$.

Selenite and selenomethionine are selenocompounds commonly found in food. Comparing their effects on proliferation, differentiation, and bone mineralization of MC3T3-E1 cells with those of Cs4-SeNPs under the same concentration (10 μM) were further investigated. In contrast to Cs4-SeNPs, the effect of selenomethionine on proliferation, differentiation, and bone mineralization of MC3T3-E1 cells did not differ significantly from those of the control (**Figs. S2-S4**). Surprisingly, selenite was found to be cytotoxic and inhibit the proliferation of MC3T3-E1 cells markedly at all time intervals (**Fig. S2**). These results collectively suggest that SeNPs with Cs4 PSP decoration is of great potential to be further developed into a novel Se source for bone health.

3.3. *Mechanistic study of the in vitro stimulating effects of Cs4-SeNPs on osteoblastic differentiation*

Cellular uptake behavior

Efficient cellular uptake of nanomaterials is a key step for exerting their biological functions (Ekkapongpisit, Giovia, Follo, Caputo, & Isidoro, 2012). As shown in Fig. 3, courmarin-6-loaded Cs4-SeNPs (10 μM) rapidly entered the MC3T3-E1 cells (about 11 min) and co-localized with lysosomes after cellular internalization, indicating that endocytosis would likely be the major cellular uptake mechanism of Cs4-SeNPs and lysosomes is their main target organelle. The involvement of endocytosis in cellular uptake of other SeNPs have been widely reported in previous literatures (G. Huang et al., 2018; Hualian Wu et al., 2012; H. Wu et al., 2013; Z. Zhang, Du, Liu, Wong, & Chen, 2019). The ability of nanoparticles uptake by cells is heavily dependent on the size and shape of nanoparticles. Shang and his co-investigators reported that individual nanoparticle with its average core size<100 nm would have higher chance to interact with cell surface receptors followed by inducing vesicle formation. Besides, spherically shaped nanoparticles could exhibit a better and quicker cellular internalization during endocytosis process (Shang et al., 2014). Therefore, it is inferred that the relatively rapid cellular uptake of Cs4-SeNPs by MC3T3-E1 cells may be attributed to their spherical shape with an average core size of approximately 30.0 nm (Fig. 1**A**).

In vitro modulation effects of Cs4-SeNPs on BMP signaling

Substantial evidence has shown that bone morphogenetic protein (BMP) signaling via Smad dependent and/or independent pathway(s) is one the most crucial signaling transduction cascades in regulating osteogenesis (Chen, Deng, & Li, 2012; Huang, Yang, Shao, & Li, 2007). In particular, distal-less homebox 5 (Dlx5), which is an upstream target of both Smad dependent and independent pathways, plays a pivotal role in activating major transcription factors [such as runt-related transcription factor 2 (Runx2) and osterix (Osx)] to regulate several downstream biomarkers for osteoblast differentiation and bone mineralization [e.g., ALP and osteocalcin (OCN)]. In BMP/Smad-dependent pathway, BMP-2 binds to cell surface receptors to form a heterotetrameric receptor complex (BMPRI or BMPRII) with the dimers of both type I and type II transmembrane serine/threonine kinases, which results in phosphorylation of Smad1/5/8 in the cytoplasm. Phosphorylated Smad1/5/8 then forms a trimetric complex with Smad4 and subsequently translocates to the nucleus. In addition, MAPKs kinases (including p38, JNK and Erk) signaling, which are upstream regulators of Dlx5 in the Smad-independant pathway, has been found to play important role in osteoblastic differentiation via regulating the Runx2, ALP and OCN expressions (Huang et al., 2007). Interestingly, we discovered that Cs4-SeNPs simultaneously activated both BMP-2/Smad dependent and independent pathways as evidenced by significant upregulation of the BMP-2 protein expression (1.46 ± 0.06 folds) as well as Smad 1/5/8 (2.00 ± 0.25 folds) and p38 (1.60 ± 0.10 folds) protein phosphorylation in the MC3T3-E1 cells after 3-day treatment [Fig. 4]. Besides, Cs4-SeNPs were found to significantly up-regulate the gene expression of those major osteogenic transcription factors [Runx2 (1.48 ± 0.06 folds); Osx (1.46 ± 0.08 folds)] as well as differentiation and mineralization biomarkers [ALP (1.77 ± 0.11 folds); OCN (2.64 ± 0.14 folds)] in the MC3T3-E1 cells [Fig. 5], further supporting their active role in promoting bone formation. The involvement of BMP/Smad signaling in other SeNPs mediated osteoblast differentiation has also been reported previously (S. Yu et al., 2018; Zheng et al., 2014).

In order to confirm the mechanistic role of BMP-2 and p38, the effect of their corresponding inhibitors, Noggin (BMP inhibitor; 100 ng/mL)

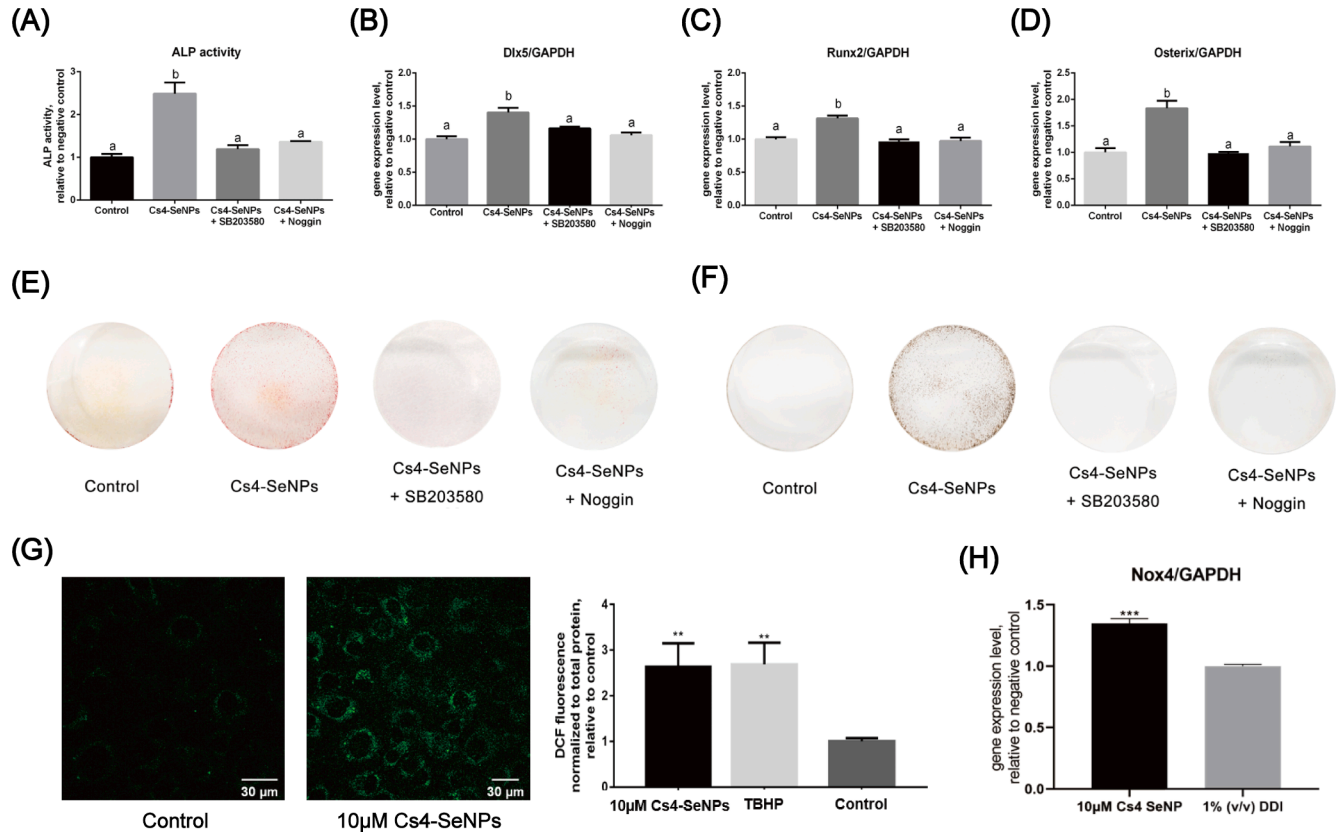

Fig. 6. Effects of BMP inhibitor (Noggin) & p38 inhibitor (SB203580) on Cs4-SeNPs mediated osteoblastic differentiation and bone mineralization as well as Cs4-SeNPs triggered Nox4-dervied intracellular ROS generation in MC3T3-E1 cells. Cells were induced with osteogenic medium for 6, 9 or 18 days with Cs4-SeNP (10 μM), Cs4-SeNP (10 μM) + Noggin (10 ng/mL), Cs4-SeNP (10 μM) + SB203580 (10 μM), or 1% (v/v) DDI (Control). (A) ALP activity of cells during differentiation process were analyzed by spectrophotometry at 405 nm. mRNA expression levels of (B) Dlx5, (C) Runx2 and (D) Osx were normalized to Control group using GAPDH as a reference. Results are mean ± SEM (n = 3). Means with different letters (a-b) are significantly different at $p < 0.05$. Calcium nodules after induction for 18 days were stained by Alizarin Red S (E) and Von Kossa (F). (G) ROS generation was determined by using DCFH-DA staining after MC3T3-E1 cells were treated with Cs4-SeNPs (10 μM) for 24 hrs. (H) MC3T3-E1 cells were treated with Cs4-SeNPs (10 μM) or 1% (v/v) DDI for 3 days, mRNA expression level of Nox4 was normalized to Control group using GAPDH as a reference. Results are mean ± SEM (n = 3). Means with "**" and "***" are significantly different at $p < 0.01$ and $p < 0.001$. (For interpretation of the references to colour in this figure legend, the reader is referred to the web version of this article.)

and SB258530 (p38 inhibitor; 10 μM) on the Cs4-SeNPs induced osteoblast differentiation and bone mineralization were further investigated. As shown in Fig. 6**A-F**, pretreatment of Noggin or SB258530 not only significantly reduced the ALP activity (45.3–52.1%) and bone nodule formation (Von Kossa and Alizarin Red S staining), but also markedly downregulated the gene expression of those major osteogenic markers such as Dlx5 (17.2–24.06%), Runx2 (26.0–26.5%) and Osx (39.3–46.2%) in osteogenesis. These findings collectively indicate that both BMP-2 and p38 play a crucial role in the BMP signaling modulated by Cs4-SeNPs.

Intracellular reactive oxygen species (ROS), mainly generated by NAD(P)H oxidases in mitochondria respiratory chain, act as a signaling mediator to play dual roles in bone homeostasis (Tao et al., 2020). Moderated intracellular ROS generation have been found to facilitate osteoblast differentiation and adhesion, while intracellular ROS overproduction would promote osteoblast apoptosis and osteoclast differentiation (Arakaki, Yamashita, Niimi, & Yamazaki, 2013; Tao et al., 2020). NAD(P)H oxidases have structurally similar catalytic subunits (Nox1-5) that are differentially expressed in various cells. Interestingly, Mandal and his co-investigators reported that BMP-2 could stimulate Nox4 intracellular ROS production at physiological level followed by promoting downstream BMP-2 gene transcription and osteoblast differentiation in murine 3T3 preosteoblast cells (Mandal et al., 2011). Similarly, in this study, we discovered that Cs4-SeNPs (10 μM) significantly triggered intracellular ROS production in MC3T3-E1 cells together with an elevation of the Nox4 gene expression after 3-day treatment [Fig. 6 **G&H**], revealing that the Cs4-SeNPs induced osteoblast differentiation would be related to Nox4-derived physiological ROS generation. It is the first study to dissect the stimulating effects of SeNPs on osteoblast differentiation and the proposed mechanism of action is schematically illustrated in Fig. 7. In short, after cellular internalization by the MC3T3-E1 cells via endocytosis, Cs4-SeNPs would trigger Nox4-derived intracellular ROS generation at physiological level followed by promoting the downstream BMP-2 gene transcription and activating the BMP signaling via both Smad dependent and Smad-independent p38 MAPK pathways.

3.4. In vivo bone protective efficacy of Cs4-SeNPs against postmenopausal osteoporosis

Ovariectomized (OVX) mouse is one of the most widely used estrogen depletion animal model to mimic the clinical condition of postmenopausal women. Compared to the sham-operated animals, ovariectomy was found to cause significant deterioration of trabecular microarchitecture of proximal femur and fifth lumbar vertebrae in OVX mice in terms of bone mineral density (BMD), bone volume/tissue volume ratio (BV/TV), trabecular number (Tb.N), thickness (Tb.Th) and separation (Tb. Sp) (Fig. 8**A&B**). Interestingly, we discovered that Cs4-SeNPs treatment (25–500 μg Se/kg BW/day) remarkably improved these bone parameters in OVX mice as evidenced by a significantly higher BMD, BV/TV, Tb. N and Tb. Th as well as significantly lower Tb. Sp (Fig. 8**A&B**). In both clinical and preclinical studies, biochemical

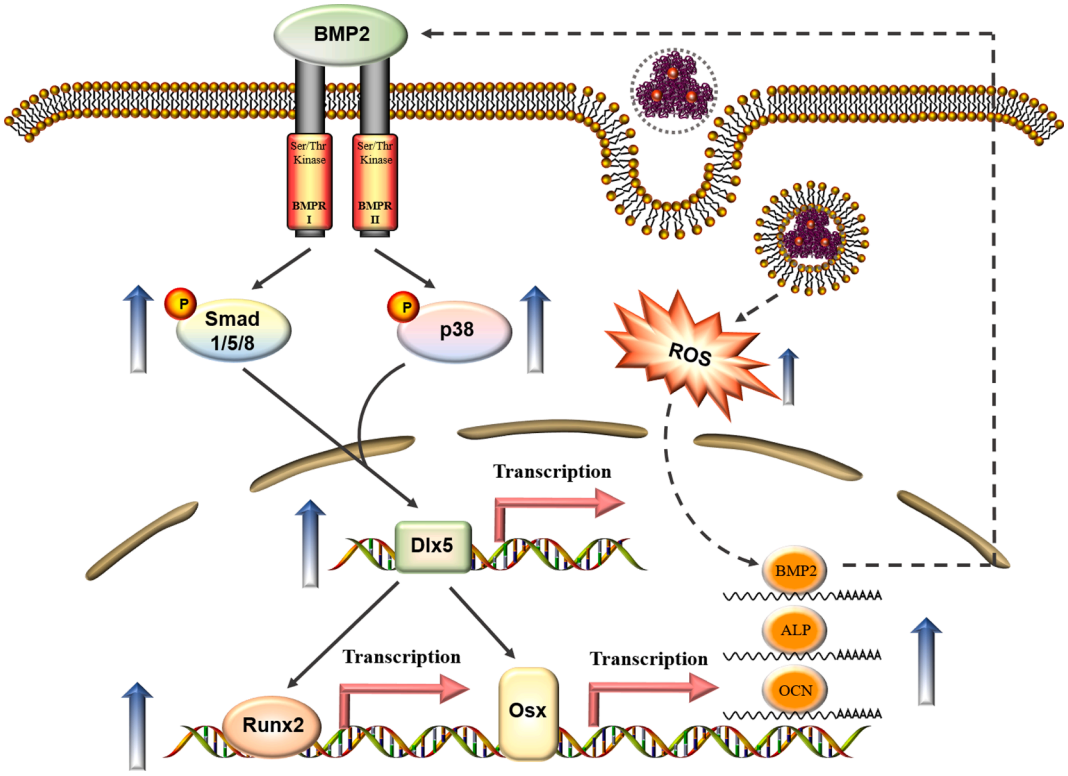

Fig. 7. A schematic of Cs4-SeNPs-triggered BMP-2/Smad signaling pathways during osteogenesis.

markers of bone turnover are crucial for assessing the effectiveness of anti-osteoporosis medications. Serum ALP level and TRAP activity are two widely used biochemical markers for bone formation and bone resorption, respectively in studying osteoporosis (Cremers & Garnero, 2006; Sørensen, Henriksen, Schaller, & Karsdal, 2007). As shown in Fig. 8**C**, further investigation on bone turnover markers reveals that Cs4-SeNPs groups (25–500 μg Se/kg BW/day) exhibited significantly higher serum ALP level (bone formation marker) as well as significantly lower serum TRAP activity (bone resorption marker) than those of the OVX model. In contrast to Runx2, mRNA expression of Osx in tibia of OVX mice fed with Cs4-SeNPs (25–500 μg Se/kg BW/day) were significantly upregulated when compared with that of the OVX group **[**Fig. 8**D]**. These findings collectively suggested that Cs4-SeNPs exhibited promising *in vivo* bone protective efficacy against OVX-induced osteoporosis via promoting bone formation, attenuating bone resorption and improving bone microarchitecture after oral gavage for 6 weeks. It is worth noting that the anti-osteoporosis efficacy of other SeNPs has been reported previously on OVX rat model, however, the effective dosage used was found to be 2–40 times higher (1 mg/kg/BW/day) (Vekariya, Kaur, & Tikoo, 2013).

Hormone replacement therapy (HRT) is a widely used treatment to relieve and prevent the physical symptoms and clinical consequences of postmenopausal osteoporosis. However, as reported by Women's Health Initiative as well as the Million Women, side effects of HRT (e.g. higher risk in developing breast, ovarian and womb cancers) are of great concern (Beral, 2003; Rossouw et al., 2002). In this study, 17β-estradiol (E2, 1 mg/g BW per day) was used as the positive control. Despite its promising anti-osteoporosis efficacy, a remarkable uterine hyperplasia was observed in the E2 group (about 7.5 times higher uterus/body weight ratio than that of OVX mice) **[**Fig. 8**E]**. It is worth noting that Cs4-SeNPs (25–500 μg Se/kg BW/day) demonstrated comparable bone protective efficacy against OVX-induced osteoporosis to that of E2, but their direct effects on uterus/body weight ratio of OVX model were insignificant **[**Fig. 8**E]**. These findings suggest that Cs4-SeNPs is relatively safe and of great potential to be further developed into a novel bone protective agent for managing postmenopausal osteoporosis.

4. Conclusion

By using mushroom PSP isolated from *Cordyceps sinensis* mycelium, novel SeNPs ("Cs4-SeNPs") with well-characterized structure and high stability were successfully prepared. Interestingly, Cs4-SeNPs (10 μM) were found to markedly induce proliferation, differentiation, and mineralization of the preosteoblast murine MC3T3-E1 cells. Further mechanistic study of Cs4-SeNPs induced osteoblast differentiation also discovered that after cellular internalization via endocytosis, Cs4-SeNPs would trigger Nox4-derived intracellular ROS generation in the MC3T3-E1 cells followed by promoting the downstream BMP-2 gene transcription and activating the BMP signaling via both Smad dependent and Smad independent p38 MAPK pathways. More importantly, Cs4-SeNPs (25–500 μg/kg BW/d) showed promising bone protective efficacy against OVX-induced osteoporosis *in vivo* via promoting bone formation, inhibiting bone resorption and improving bone microarchitecture after oral gavage for 6 weeks. Findings of this study collectively suggested that Cs4-SeNPs is of great potential to be further developed into a safe and evidence-based nano-mineral for managing postmenopausal osteoporosis. Further investigation on their gastro-intestinal stability, biodistribution, metabolism, and toxicity by using different cell and animal models is now underway.

CRediT authorship contribution statement

Kar-Him Luk: Investigation, Methodology, Formal analysis. **Cheuk-Hin Chan:** Investigation, Data curation. **Zhi-Wen Liu:** Data curation, Visualization. **Chun-Wei Jiao:** Writing - Review & Editing. **Xiao-Bing Yang:** Writing - Review & Editing. **Xiao-Li Dong:** Writing - Original Draft, Supervision, Project administration. **Ka-Hing Wong:** Writing - Review & Editing, Supervision,Funding acquisition.

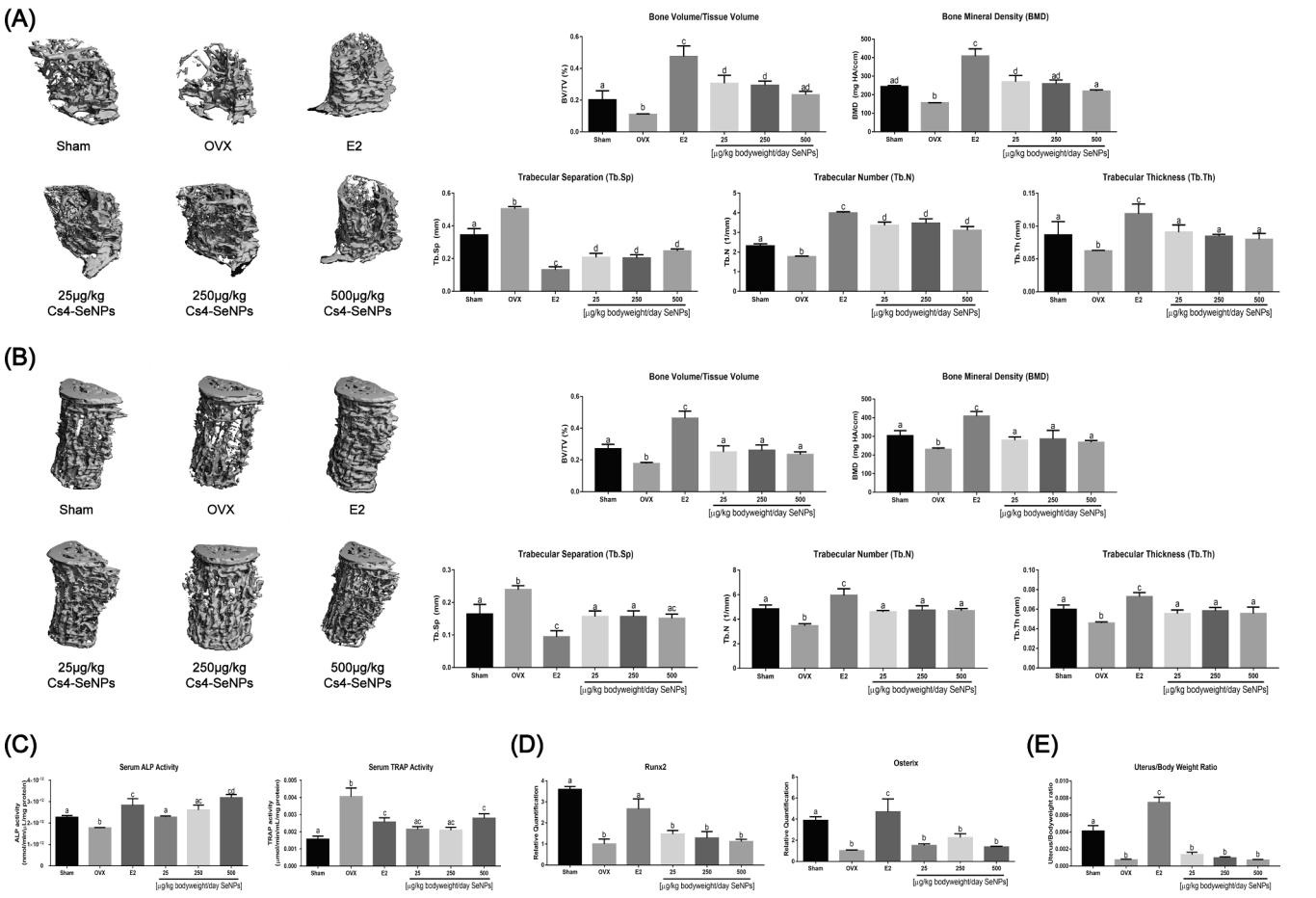

Fig. 8. In vivo bone protective efficacy of Cs4-SeNPs against ovariectomy-induced osteoporosis. 3-month-old mature, female C57BL/6J mice (OVX or sham operated) were orally administrated with Cs4-SeNPs (25, 250 and 500 μg Se/kg BW/day) or 17β-estradiol (E2; 1 mg/g BW per day positive control) for a total of 6 weeks. (A) Representative 3D reconstructed image, BMD, BV/TV as well as Tb.Th, Tb.N and Tb. Sp of proximal femur was obtained by MicroCT analysis. (B) Representative 3D reconstructed image, BMD, BV/TV as well as Tb.Th, Tb.N and Tb. Sp of fifth lumbar vertebra was obtained by Micro-CT analysis. (C) Bone turnover markers such as serum ALP (bone formation marker) and TRAP (bone resorption marker) were evaluated using colorimetric assay kits. (D) mRNA expression of Runx2 and Osx in tibia was determined by real time-PCR and normalized to that of β-actin. (E) Uterus/body weight ratio. Results are mean ± SEM (n = 8). Means with different letters (a-d) are significantly different ($p < 0.05$; one-way ANOVA).

Declaration of Competing Interest

The authors declare that they have no known competing financial interests or personal relationships that could have appeared to influence the work reported in this paper.

Data availability

Data will be made available on request.

Acknowledgements

This work was supported by International Scientific and Technological Cooperation Project of Guangzhou Development Zone (grant number: 2020GH07); Key Project of Shenzhen Basic Research Program (grant number: JCYJ20200109142019319); Collabortaive Innovation and Platform Establsihment Project of Department of Science and Technology of Guangdong Province (grant number: 2019A050520003); Collaborative Research Project of Innovation and Technology Support Program (grant number: ITS/258/15FX); Dean's Reserve of The Hong Kong Polytechnic University (grant number: ZVN7); Interdisciplinary Project Fund of Research Institute for Future Food, The Hong Kong Polytechnic University (grant number: 1-CD60).

The abstract of this paper was presented at the European Assembly of Advanced Materials Congress online as a conference talk with interim findings (28-31 August 2022; Stockholm, Sweden)

Appendix A. Supplementary data

Supplementary data to this article can be found online at https://doi.org/10.1016/j.jff.2023.105832.

References

An, K. C. (2016). Selective estrogen receptor modulators. *Asian Spine J, 10*(4), 787–791. https://doi.org/10.4184/asj.2016.10.4.787

Anagnostis, P., Paschou, S. A., Mintziori, G., Ceausu, I., Depypere, H., Lambrinoudaki, I., … Goulis, D. G. (2017). Drug holidays from bisphosphonates and denosumab in postmenopausal osteoporosis: EMAS position statement. *Maturitas, 101*, 23–30. https://doi.org/10.1016/j.maturitas.2017.04.008

Arakaki, N., Yamashita, A., Niimi, S., & Yamazaki, T. (2013). Involvement of reactive oxygen species in osteoblastic differentiation of MC3T3-E1 cells accompanied by mitochondrial morphological dynamics. *Biomedical Research, 34*(3), 161–166. https://doi.org/10.2220/biomedres.34.161

Beral, V. (2003). Breast cancer and hormone-replacement therapy in the Million Women Study. *Lancet, 362*(9382), 419–427. https://doi.org/10.1016/s0140-6736(03)14065-2

Black, D. M., & Rosen, C. J. (2016). Clinical practice. Postmenopausal osteoporosis. *N Engl J Med, 374*(3), 254–262. https://doi.org/10.1056/NEJMcp1513724

Cao, J. J., Gregoire, B. R., & Zeng, H. (2012). Selenium deficiency decreases antioxidative capacity and is detrimental to bone microarchitecture in mice. *The Journal of Nutrition, 142*(8), 1526–1531. https://doi.org/10.3945/jn.111.157040

Chaudhary, S., Umar, A., & Mehta, S. K. (2014). Surface functionalized selenium nanoparticles for biomedical applications. *Journal of Biomedical Nanotechnology, 10* (10), 3004–3042. https://doi.org/10.1166/jbn.2014.1985

Chen, G., Deng, C., & Li, Y. P. (2012). TGF-β and BMP signaling in osteoblast differentiation and bone formation. *International Journal of Biological Sciences, 8*(2), 272–288. https://doi.org/10.7150/ijbs.2929

Compston, J. E., McClung, M. R., & Leslie, W. D. (2019). Osteoporosis. *Lancet, 393* (10169), 364–376. https://doi.org/10.1016/s0140-6736(18)32112-3

Cremers, S., & Garnero, P. (2006). Biochemical markers of bone turnover in the clinical development of drugs for osteoporosis and metastatic bone disease: Potential uses and pitfalls. *Drugs, 66*(16), 2031–2058. https://doi.org/10.2165/00003495-200666160-00001

Ebert, R., & Jakob, F. (2007). Selenium deficiency as a putative risk factor for osteoporosis. *International Congress Series, 1297*, 158–164. https://doi.org/10.1016/j.ics.2006.08.001

Ebert, R., Ulmer, M., Zeck, S., Meissner-Weigl, J., Schneider, D., Stopper, H., … Jakob, F. (2006). Selenium supplementation restores the antioxidative capacity and prevents cell damage in bone marrow stromal cells in vitro. *Stem Cells, 24*(5), 1226–1235. https://doi.org/10.1634/stemcells.2005-0117

Ekkapongpisit, M., Giovia, A., Follo, C., Caputo, G., & Isidoro, C. (2012). Biocompatibility, endocytosis, and intracellular trafficking of mesoporous silica and polystyrene nanoparticles in ovarian cancer cells: Effects of size and surface charge groups. *International Journal of Nanomedicine, 7*, 4147–4158. https://doi.org/10.2147/ijn.S33803

Esbrit, P., Herrera, S., Portal-Núñez, S., Nogués, X., & Díez-Pérez, A. (2016). Parathyroid hormone-related protein analogs as osteoporosis therapies. *Calcified Tissue International, 98*(4), 359–369. https://doi.org/10.1007/s00223-015-0050-1

Ferro, C., Florindo, H. F., & Santos, H. A. (2021). Selenium nanoparticles for biomedical applications: from development and characterization to therapeutics. *Advanced Healthcare Materials, 10*(16), e2100598.

Huang, G., Liu, Z., He, L., Luk, K. H., Cheung, S. T., Wong, K. H., & Chen, T. (2018). Autophagy is an important action mode for functionalized selenium nanoparticles to exhibit anti-colorectal cancer activity. *Biomaterials Science, 6*(9), 2508–2517. https://doi.org/10.1039/c8bm00670a

Huang, L., Wang, X., Cao, H., Li, L., Chow, D. H., Tian, L., … Qin, L. (2018). A bone-targeting delivery system carrying osteogenic phytomolecule icaritin prevents osteoporosis in mice. *Biomaterials, 182*, 58–71. https://doi.org/10.1016/j.biomaterials.2018.07.046

Huang, W., Yang, S., Shao, J., & Li, Y. P. (2007). Signaling and transcriptional regulation in osteoblast commitment and differentiation. *Frontiers in Bioscience: a Journal and Virtual Library, 12*, 3068–3092. https://doi.org/10.2741/2296

Kim, B. S., Kang, H. J., Park, J. Y., & Lee, J. (2015). Fucoidan promotes osteoblast differentiation via JNK- and ERK-dependent BMP2-Smad 1/5/8 signaling in human mesenchymal stem cells. *Experimental & Molecular Medicine, 47*(1), e128.

Lee, S. C., Lee, N. H., Patel, K. D., Jang, T. S., Knowles, J. C., Kim, H. W., . . . Lee, J. H. (2021). The effect of selenium nanoparticles on the osteogenic differentiation of MC3T3-E1 cells. *Nanomaterials (Basel), 11*(2). doi: 10.3390/nano11020557.

Liu, H., Bian, W., Liu, S., & Huang, K. (2012). Selenium protects bone marrow stromal cells against hydrogen peroxide-induced inhibition of osteoblastic differentiation by suppressing oxidative stress and ERK signaling pathway. *Biological Trace Element Research, 150*(1–3), 441–450. https://doi.org/10.1007/s12011-012-9488-4

Lorentzon, M., Johansson, H., Harvey, N. C., Liu, E., Vandenput, L., McCloskey, E. V., & Kanis, J. A. (2022). Osteoporosis and fractures in women: The burden of disease. *Climacteric, 25*(1), 4–10. https://doi.org/10.1080/13697137.2021.1951206

Mandal, C. C., Ganapathy, S., Gorin, Y., Mahadev, K., Block, K., Abboud, H. E., … Ghosh-Choudhury, N. (2011). Reactive oxygen species derived from Nox4 mediate BMP2 gene transcription and osteoblast differentiation. *Biochemical Journal, 433*(2), 393–402. https://doi.org/10.1042/bj20100357

Moreno-Reyes, R., Egrise, D., Nève, J., Pasteels, J. L., & Schoutens, A. (2001). Selenium deficiency-induced growth retardation is associated with an impaired bone metabolism and osteopenia. *Journal of Bone and Mineral Research, 16*(8), 1556–1563. https://doi.org/10.1359/jbmr.2001.16.8.1556

Moreno-Reyes, R., Mathieu, F., Boelaert, M., Begaux, F., Suetens, C., Rivera, M. T., … Vanderpas, J. (2003). Selenium and iodine supplementation of rural Tibetan children affected by Kashin-Beck osteoarthropathy. *The American Journal of Clinical Nutrition, 78*(1), 137–144. https://doi.org/10.1093/ajcn/78.1.137

Notelovitz, M. (1997). Estrogen therapy and osteoporosis: Principles & practice. *The American Journal of the Medical Sciences, 313*(1), 2–12. https://doi.org/10.1097/00000441-199701000-00002

Qi, W., Yan, Y. B., Lei, W., Wu, Z. X., Zhang, Y., Liu, D., … Liu, N. (2012). Prevention of disuse osteoporosis in rats by Cordyceps sinensis extract. *Osteoporosis International (London), 23*(9), 2347–2357. https://doi.org/10.1007/s00198-011-1842-4

Rayman, M. P. (2000). The importance of selenium to human health. *Lancet, 356*(9225), 233–241. https://doi.org/10.1016/s0140-6736(00)02490-9

Rossouw, J. E., Anderson, G. L., Prentice, R. L., LaCroix, A. Z., Kooperberg, C., Stefanick, M. L., … Ockene, J. (2002). Risks and benefits of estrogen plus progestin in healthy postmenopausal women: Principal results From the Women's Health Initiative randomized controlled trial. *Journal of the American Medical Association, 288*(3), 321–333. https://doi.org/10.1001/jama.288.3.321

Shang, L., Nienhaus, K., Jiang, X., Yang, L., Landfester, K., Mailänder, V., … Nienhaus, G. U. (2014). Nanoparticle interactions with live cells: Quantitative fluorescence microscopy of nanoparticle size effects. *Beilstein Journal of Nanotechnology, 5*, 2388–2397. https://doi.org/10.3762/bjnano.5.248

Shashidhar, G. M., Giridhar, P., & Manohar, B. (2015). Functional polysaccharides from medicinal mushroom Cordyceps sinensis as a potent food supplement: extraction, characterization and therapeutic potentials – a systematic review. [10.1039/C4RA13539C]. *RSC Advances, 5*(21), 16050-16066. doi: 10.1039/C4RA13539C.

Sikon, A., & Batur, P. (2010). Profile of teriparatide in the management of postmenopausal osteoporosis. *International Journal of Women's Health, 2*, 37–44. https://doi.org/10.2147/ijwh.s4919

Sørensen, M. G., Henriksen, K., Schaller, S., & Karsdal, M. A. (2007). Biochemical markers in preclinical models of osteoporosis. *Biomarkers, 12*(3), 266–286. https://doi.org/10.1080/13547500601070842

Tao, H., Ge, G., Liang, X., Zhang, W., Sun, H., Li, M., & Geng, D. (2020). ROS signaling cascades: Dual regulations for osteoclast and osteoblast. *Acta Biochimica et Biophysica Sinica (Shanghai), 52*(10), 1055–1062. https://doi.org/10.1093/abbs/gmaa098

Vekariya, K. K., Kaur, J., & Tikoo, K. (2013). Alleviating anastrozole induced bone toxicity by selenium nanoparticles in SD rats. *Toxicology and Applied Pharmacology, 268*(2), 212–220. https://doi.org/10.1016/j.taap.2013.01.028

Wang, H., Zhang, J., & Yu, H. (2007). Elemental selenium at nano size possesses lower toxicity without compromising the fundamental effect on selenoenzymes: Comparison with selenomethionine in mice. *Free Radical Biology & Medicine, 42*(10), 1524–1533. https://doi.org/10.1016/j.freeradbiomed.2007.02.013

Wang, X., He, Y., Guo, B., Tsang, M. C., Tu, F., Dai, Y., … Qin, L. (2015). In vivo screening for anti-osteoporotic fraction from extract of herbal formula Xianlinggubao in ovariectomized mice. *PLoS One1, 10*(2), e0118184.

Wu, H., li, X., Liu, W., Chen, T., Li, Y., Zheng, W., . . . Wong, K. H. (2012). Surface decoration of selenium nanoparticles by mushroom polysaccharides–protein complexes to achieve enhanced cellular uptake and antiproliferative activity. J. Mater. Chem., 22, 9602-9610. doi: 10.1039/C2JM16828F.

Wu, H., Zhu, H., Li, X., Liu, Z., Zheng, W., Chen, T., … Wong, K. H. (2013). Induction of apoptosis and cell cycle arrest in A549 human lung adenocarcinoma cells by surface-capping selenium nanoparticles: An effect enhanced by polysaccharide-protein complexes from Polyporus rhinocerus. *Journal of Agricultural and Food Chemistry, 61* (41), 9859–9866. https://doi.org/10.1021/jf403564s

Yan, J. K., Wang, W. Q., & Wu, J. Y. (2014). Recent advances in Cordyceps sinensis polysaccharides: Mycelial fermentation, isolation, structure, and bioactivities: A review. *Journal of Functional Foods, 6*, 33–47. https://doi.org/10.1016/j.jff.2013.11.024

Yu, B., Zhang, Y., Zheng, W., Fan, C., & Chen, T. (2012). Positive surface charge enhances selective cellular uptake and anticancer efficacy of selenium nanoparticles. *Inorganic Chemistry, 51*(16), 8956–8963. https://doi.org/10.1021/ic301050v

Yu, S., Luk, K. H., Cheung, S. T., Kwok, K. W., Wong, K. H., & Chen, T. (2018). Polysaccharide-protein complex-decorated selenium nanosystem as an efficient bone-formation therapeutic. *Journal of Materials Chemistry B, 6*(32), 5215–5219. https://doi.org/10.1039/c8tb01084f

Zeng, D., Zhao, J., Luk, K. H., Cheung, S. T., Wong, K. H., & Chen, T. (2019). Potentiation of in vivo anticancer efficacy of selenium nanoparticles by mushroom polysaccharides surface decoration. *Journal of Agricultural and Food Chemistry, 67* (10), 2865–2876. https://doi.org/10.1021/acs.jafc.9b00193

Zhang, J., Wang, H., Yan, X., & Zhang, L. (2005). Comparison of short-term toxicity between Nano-Se and selenite in mice. *Life Sciences, 76*(10), 1099–1109. https://doi.org/10.1016/j.lfs.2004.08.015

Zhang, Z., Du, Y., Liu, T., Wong, K. H., & Chen, T. (2019). Systematic acute and subchronic toxicity evaluation of polysaccharide-protein complex-functionalized selenium nanoparticles with anticancer potency. *Biomaterials Science, 7*(12), 5112–5123. https://doi.org/10.1039/c9bm01104h

Zheng, C., Wang, J., Liu, Y., Qianqian, y., Liu, Y., Deng, N., & Liu, J. (2014). Functional selenium nanoparticles enhanced stem cell osteoblastic differentiation through BMP signaling pathways. *Advanced Functional Materials, 24*. doi: 10.1002/adfm.201401263.

Zhu, J. S., Halpern, G. M., & Jones, K. (1998a). The scientific rediscovery of a precious ancient Chinese herbal regimen: Cordyceps sinensis: Part II. *Journal of Alternative and Complementary Medicine, 4*(4), 429–457. https://doi.org/10.1089/acm.1998.4.429

Zhu, J. S., Halpern, G. M., & Jones, K. (1998b). The scientific rediscovery of an ancient Chinese herbal medicine: Cordyceps sinensis: Part I. *Journal of Alternative and Complementary Medicine, 4*(3), 289–303. https://doi.org/10.1089/acm.1998.4.3-289